

# An Aluminophosphate of Molybdenum (V) with a Tunnel Structure: $\text{Cs}_9\text{Mo}_9\text{Al}_3\text{P}_{11}\text{O}_{59}$

A. Guesdon, M. M. Borel, A. Leclaire, A. Grandin, and B. Raveau

*Laboratoire CRISMAT, CNRS URA 1318 ISMRA, Université de Caen, Boulevard du Maréchal Juin, 14050 Caen Cedex, France*

Received January 18, 1994; in revised form April 20, 1994; accepted May 7, 1994

A new Mo(V) aluminophosphate,  $\text{Cs}_9\text{Mo}_9\text{Al}_3\text{P}_{11}\text{O}_{59}$ , has been isolated. This hexagonal phase ( $P6_3/m$ ;  $a = 16.989(3)$  Å,  $c = 11.866(3)$  Å) exhibits a tunnel-type structure with a host lattice that is composed of  $\text{MoO}_6$  octahedra and  $\text{AlO}_4$  and  $\text{PO}_4$  tetrahedra. In fact, this open framework can be described in terms of tetrahedral  $\text{Al}_3\text{P}_{10}\text{O}_{40}$  units and octahedral  $\text{Mo}_3\text{O}_{15}$  units. The latter consist of two edge-sharing octahedra sharing one of their common apices with one  $\text{MoO}_6$  octahedron. Such units form  $[\text{AlMo}_3\text{P}_3\text{O}_{22}]_\infty$  columns running along  $c$ . The assemblage of these columns through the apices of their polyhedra but also through single monophosphate groups leads to the  $[\text{Mo}_9\text{Al}_3\text{P}_{11}\text{O}_{59}]_\infty$  host lattice with tunnels running along  $c$  where the cesium cations are located. The relationships between this structure and those of carnegite and  $\text{Cs}_8\text{Mo}_7\text{O}_9(\text{PO}_4)_7 \cdot \text{H}_2\text{O}$  are discussed. © 1995 Academic Press, Inc.

## INTRODUCTION

The stabilization of Mo(V) in a phosphate matrix has allowed the synthesis of a various number of mixed frameworks, exhibiting open structures owing to the specific geometry of the Mo(V) octahedron that exhibits one free apex. More than 30 different new phosphates of pentavalent molybdenum have been isolated within the past few years (for review, see Refs. 1, 2). The introduction of aluminium into the phosphorous sites allow new open frameworks to be generated, keeping in mind the well-known aluminosilicates with zeolitic properties. Moreover, the latter element may introduce greater flexibility for the creation of new structures since it is able to adopt both tetrahedral and octahedral coordinations. The exploration of the Mo(V) aluminophosphates that we have just started is based on these considerations. We report here on the synthesis and crystal structure of a new aluminophosphate of pentavalent molybdenum,  $\text{Cs}_9\text{Mo}_9\text{Al}_3\text{P}_{11}\text{O}_{59}$ , that exhibits a tunnel-type structure.

## SAMPLE PREPARATION AND CRYSTAL GROWTH

The molybdenum V aluminophosphate  $\text{Cs}_9\text{Mo}_9\text{Al}_3\text{P}_{11}\text{O}_{59}$  was prepared in powder form in two steps. In the first

step, a mixture of  $\text{H}(\text{NH}_4)_2\text{PO}_4$ ,  $\text{Al}(\text{NO}_3)_3 \cdot 9\text{H}_2\text{O}$ ,  $\text{CsNO}_3$ , and  $\text{MoO}_3$  was heated to 673 K in air in order to decompose the nitrate and the ammonium phosphate. In the second step, the resulting finely ground powder was mixed with the appropriate amount of molybdenum (0.66 mole). This sample, placed in an alumina tube, was sealed in an evacuated silica ampoule, heated to 1000 K for 2 days, and quenched at room temperature. The result was a brown powder.

The powder X-ray diffractogram determined with a PW3710 Philips diffractometer was indexed in a hexagonal cell (Table 1) in agreement with the parameters obtained from the single crystal structure.

The single crystals were extracted from the composition  $\text{Cs}_9\text{Mo}_9\text{Al}_3\text{P}_{11}\text{O}_{59}$ . The crystal growth was performed in two steps in a manner similar to that described above but the sample was heated to 1050 K for 1 day, then slowly cooled at  $2 \text{ K} \cdot \text{hr}^{-1}$  to 920 K, and finally quenched at room temperature. Several orange single crystals were extracted from the latter sample. The microprobe analysis of those crystals indicated the elements Cs, Mo, Al, and P with molar ratios corresponding to the composition " $\text{Cs}_9\text{Mo}_9\text{Al}_3\text{P}_{11}$ ," in agreement with the refinement of the crystal structure.

## STRUCTURE DETERMINATION

An orange crystal with dimensions  $0.116 \times 0.109 \times 0.090$  mm was selected for the structure determination. The cell parameters reported in Table 2 were determined and refined by using diffractometric techniques at 294 K with a least-squares refinement based upon 25 reflections with  $18^\circ < \theta < 22^\circ$ . The systematic absence  $l = 2n + 1$  for  $00l$  led to two possible space groups;  $P6_3$  and  $P6_3/m$ . The structure determination was successful in the centrosymmetric group  $P6_3/m$  (No. 176). The data were collected with a CAD4 Enraf-Nonius diffractometer with the data collection parameters given in Table 2. The reflections were corrected for Lorentz and polarization effects; no absorption corrections were performed. The

TABLE 1  
Interreticular Distances

<i>h k l</i>	$d_{\text{calc}}$ (Å)	$d_{\text{obs}}$ (Å)	<i>I</i>	<i>h k l</i>	$d_{\text{calc}}$ (Å)	$d_{\text{obs}}$ (Å)	<i>I</i>
0 1 0	14.71	14.69	2	0 3 5	2.14	2.13	1
0 1 1	9.24	9.23	7	0 7 0	2.10	2.10	3
1 1 0	8.50	8.50	10	3 5 0	2.10		
0 2 0	7.36	7.36	15	1 6 2	2.10		
1 1 1	6.91	6.91	29	0 6 3	2.08	2.08	2
0 2 1	6.25	6.26	1	2 2 5	2.07	2.07	4
0 0 2	5.93	5.92	3	0 7 1	2.07		
1 2 0	5.56	5.57	5	3 5 1	2.07		
0 1 2	5.50	5.49	10	3 4 3	2.06	2.06	5
1 2 1	5.04	5.04	5	2 6 0	2.04	2.04	3
0 3 0	4.90	4.91	5	2 5 3	2.02	2.02	2
0 2 2	4.62	4.61	2	4 4 2	2.00	2.00	1
0 3 1	4.53	4.54	3	0 4 5	1.99		
2 2 0	4.25	4.25	8	0 7 2	1.98	1.98	2
1 3 0	4.08	4.09	16	3 5 2	1.98		
1 2 2	4.06	4.05	14	0 0 6	1.98		
2 2 1	4.00	4.00	16	1 5 4	1.97	1.97	2
1 3 1	3.86	3.86	16	1 6 3	1.95	1.95	5
0 1 3	3.82	3.81	2	1 7 0	1.949		
0 4 0	3.68	3.68	1	2 3 5	1.94	1.94	5
0 2 3	3.48	3.48	12	2 6 2	1.93	1.93	4
1 3 2	3.36	3.36	74	1 1 6	1.93	1.92	5
2 3 1	3.25	3.25	10	1 7 1	1.92		
1 4 0	3.21	3.21	100	0 6 4	1.89	1.89	2
0 4 2	3.13	3.13	12	4 5 0	1.88	1.88	2
1 4 1	3.10	3.10	11	3 4 4	1.88	1.87	1
0 3 3	3.08	3.08	7	4 4 3	1.87		
0 0 4	2.97	2.96	4	1 2 6	1.86	1.86	5
2 3 2	2.93	2.93	4	4 5 1	1.86		
0 1 4	2.91	2.90	2	0 7 3	1.86	1.86	6
0 5 1	2.86	2.86	3	3 5 3	1.86		
1 3 3	2.84	2.84	5	3 6 0	1.85		
1 4 2	2.82	2.82	7	2 5 4	1.85	1.84	6
2 4 0	2.78	2.78	5	0 8 0	1.84	1.84	3
3 3 1	2.75	2.75	1	0 3 6	1.83	1.83	4
0 2 4	2.75			3 6 1	1.83		
2 4 1	2.71	2.71	1	3 3 5	1.82	1.82	3
0 4 3	2.69	2.69	6	0 8 1	1.82		
0 5 2	2.64	2.64	2	2 6 3	1.81	1.81	3
1 2 4	2.62	2.61	3	2 4 5	1.81	1.80	9
1 5 1	2.58	2.58	11	2 7 0	1.80	1.80	8
0 3 4	2.54	2.54	4	1 5 5	1.77	1.77	4
2 4 2	2.52	2.52	2	0 8 2	1.76	1.76	5
1 4 3	2.49	2.49	1	4 4 4	1.73	1.73	2
0 6 0	2.45	2.45	1	1 8 0	1.72	1.72	2
1 5 2	2.41	2.41	8	2 7 2	1.72		
1 3 4	2.40	2.40	7	0 7 4	1.72	1.72	4
3 4 1	2.37	2.37	10	3 5 4	1.72		
2 5 0	2.36	2.36	9	2 3 6	1.71	1.71	4
0 1 5	2.34	2.34	5	0 6 5	1.71		
2 5 1	2.31	2.31	4	1 8 1	1.70		
1 1 5	2.29	2.28	4	4 5 3	1.70	1.70	2
2 4 3	2.28	2.28	7	5 5 0	1.70		
0 6 2	2.27	2.27	4	4 6 0	1.69	1.69	1
3 4 2	2.24	2.24	5	5 5 1	1.68	1.68	3
1 5 3	2.20	2.20	2	2 6 4	1.68		
2 5 2	2.19	2.19	3	3 6 3	1.68		
1 2 5	2.18	2.18	5	2 5 5	1.67	1.67	4
1 4 4	2.18			4 6 1	1.67		

TABLE 1—Continued

<i>h k l</i>	$d_{\text{calc}}$ (Å)	$d_{\text{obs}}$ (Å)	<i>I</i>	<i>h k l</i>	$d_{\text{calc}}$ (Å)	$d_{\text{obs}}$ (Å)	<i>I</i>
0 8 3	1.67	1.67	2	1 7 4	1.63		
3 7 0	1.66	1.66	1	4 6 2	1.62	1.63	3
1 8 2	1.65			1 2 7	1.62	1.62	1
2 7 3	1.64	1.64	3	3 3 6	1.62		
0 9 0	1.64			0 9 1	1.62		
1 6 5	1.63	1.63	6				

structure was solved with the heavy atom method. The resolution and the refinement of the structure were carried out with the S.D.P. chain program of B. A. Frenz & Associates Inc. (1982), SDP Structure Determination Package, College Station, TX. The refinement of atomic coordinates and anisotropic thermal factors led to  $R = 0.034$  and  $R_w = 0.033$  and to the atomic parameters presented in Table 3. Note the rather high  $B_{\text{eq}}$  factors of several oxygen atoms that have in fact been refined anisotropically. This can be explained for O(6), O(13), and O(15) by the fact that these atoms correspond to the free apices of the Mo(2), P(3), and P(4) polyhedra, respec-

TABLE 2  
Summary of Crystal Data, Intensity Measurements, and Structure Refinement Parameters for  $\text{Cs}_9\text{Mo}_9\text{Al}_3\text{P}_{11}\text{O}_{59}$

1 Crystal data	
Space group	$P6_3/m$
Cell dimensions	$a = b = 16.989(3)$ Å $c = 11.866(3)$ Å
Volume	$2966(2)$ Å <sup>3</sup>
<i>Z</i>	2
$d_{\text{calc}}$	3.84
$d_{\text{exp}}$	3.88
2 Intensity measurements	
$\lambda(\text{MoK}\alpha)$	0.71073 Å
Scan mode	$\omega - \theta$
Scan width (°)	$1 + 0.35 \tan \theta$
Slit aperture (mm)	$1.0 + \tan \theta$
Max $\theta$ (°)	45°
Measured reflections	8942
Standard reflections	3 (every 3000 sec)
Reflections with $I > 3\sigma$	2040
$\mu(\text{mm}^{-1})$	7.66
Structure solution and refinement	
Parameters refined	164
Agreement factors	$R = 0.034, R_w = 0.033$
Weighting scheme	$w = f(\sin \theta/\lambda)^a$
$\Delta/\sigma$ max	<0.004
$\Delta\rho$ (eÅ <sup>-3</sup> )	<2.7

<sup>a</sup> The  $w$  are a function of  $\sin \theta/\lambda$  deduced from the analysis of the variances of the  $F_0$  made with an adaptation of the computer program HANOVA of W. C. Hamilton quoted in the paper of S. C. Abrahams, L. E. Alexander, T. C. Furnas, W. C. Hamilton, J. Ladell, Y. Okaya, R. A. Young and A. Zalkin, *Acta Crystallogr.* **22**, 1 (1967).

TABLE 3  
Positional Parameters and Their Estimated Standard Deviations

Atom	<i>x</i>	<i>y</i>	<i>z</i>	<i>B</i> (Å <sup>2</sup> )	Occupancy
Cs(1)	0.14693(3)	0.52752(3)	0.45383(5)	2.853(9)	1
Cs(2)	0.02678(5)	0.19754(6)	0.2644(2)	3.72(3)	0.5
Mo(1)	0.27147(5)	0.44017(5)	0.25	0.77(1)	1
Mo(2)	0.27908(3)	0.23409(3)	0.36040(5)	0.898(8)	1
P(1)	0.4469(1)	0.4138(2)	0.25	0.94(4)	1
P(2)	0.3778(1)	0.1280(1)	0.4817(1)	0.86(3)	1
P(3)	0.66667	0.33333	0.7138(5)	1.01(7)	0.5
P(4)	0.33333	0.66667	0.7057(6)	1.50(9)	0.5
Al	0.4873(2)	0.1551(2)	0.25	0.95(5)	1
O(1)	0.1607(4)	0.4063(5)	0.25	1.6(1)	1
O(2)	0.3169(5)	0.5747(5)	0.25	2.5(2)	1
O(3)	0.2534(4)	0.3114(4)	0.25	1.0(1)	1
O(4)	0.2857(3)	0.4460(3)	0.4189(4)	1.24(9)	1
O(5)	0.4124(4)	0.4822(4)	0.25	1.1(1)	1
O(6)	0.1699(4)	0.1494(3)	0.3759(5)	2.1(1)	1
O(7)	0.2713(3)	0.3025(3)	0.5014(5)	1.63(9)	1
O(8)	0.3402(3)	0.1924(3)	0.4757(4)	1.45(9)	1
O(9)	0.3193(5)	0.1793(4)	0.25	1.6(1)	1
O(10)	0.4130(3)	0.3543(3)	0.3554(4)	1.38(9)	1
O(11)	0.5509(4)	0.4687(5)	0.25	1.9(2)	1
O(12)	0.4308(3)	0.1318(3)	0.3777(4)	1.8(1)	1
O(13)	0.66667	0.33333	0.588(2)	2.0(3)	0.5
O(14)	0.3055(5)	0.5722(5)	0.75	2.5(2)	1
O(15)	0.33333	0.66666	0.579(2)	3.8(4)	0.5

Note. Anisotropically refined atoms are given in the form of the isotropic equivalent displacement parameter defined as:  $B = 4/3 [\beta_{11}a^2 + \beta_{22}b^2 + \beta_{33}c^2 + \beta_{12}ab \cos \gamma + \beta_{13}ac \cos \beta + \beta_{23}bc \cos \alpha]$ .

tively. In the case of O(2) and O(14), it is likely that these atoms do not sit exactly at  $z = 1/4$ , i.e., in the mirror, but are split randomly on both sites of the mirror. The *B* values of cesium ranging from 2.8 to 3.7 Å are similar to those often observed for this cation, as it is located in the tunnels. Note that in the latter case, the *B* value increases with the mean value of the Cs–O distances, i.e., with the size of the tunnel.

#### DESCRIPTION OF THE STRUCTURE AND DISCUSSION

The projection of the structure along *c* (Fig. 1) shows that the  $[\text{Mo}_9\text{Al}_3\text{P}_{11}\text{O}_{59}]_x$  host lattice is composed of single  $\text{PO}_4$  and  $\text{AlO}_4$  tetrahedra sharing their apices with  $\text{MoO}_6$  octahedra. This framework delimits two sorts of tunnels running along *c*: large tunnels where Cs(2) cations are located, and smaller tunnels containing Cs(1) cations.

The first important feature deals with the presence of “ $\text{Mo}_3\text{O}_{15}$ ” octahedral units (Fig. 2) that consist of two edge-sharing  $\text{MoO}_6$  octahedra (Mo(2) sharing one of their common apices with a Mo(1) octahedron, leading to one oxygen atom being triply bonded (O(3))). Such “ $\text{Mo}_3\text{O}_{15}$ ” units have already been observed on the mixed va-

lent Mo(IV)–Mo(V) phosphate  $\text{Cs}_6\text{Mo}_7\text{O}_9(\text{PO}_4)_7 \cdot \text{H}_2\text{O}$  (Ref. 3).

Each of these  $\text{MoO}_6$  octahedra exhibits one free oxygen apex characteristic of Mo(V) and directed toward the center of the largest tunnels (Fig. 1). Consequently, the geometry of these two kinds of  $\text{MoO}_6$  octahedra is characterized by a short molybdenyl Mo–O bond of 1.67 Å for Mo(1) and 1.696 Å for Mo(2), the opposite bond being abnormally long (2.129 and 2.17 Å for Mo(1) and Mo(2), respectively), whereas the four other equatorial Mo–O distances are rather homogeneous, ranging from 2.014 to 2.051 Å for Mo(1) and from 1.92 to 2.079 Å for Mo(2) (Table 4). The valence bond calculations confirm the pentavalence of molybdenum since the Zachariasen model (4) leads to a valence of 5.1 for Mo(1) and 4.9 for Mo(2).

The second interesting characteristic of this framework deals with the existence of “ $\text{Al}_3\text{P}_{10}\text{O}_{40}$ ” tetrahedral units built up from 3  $\text{AlO}_4$  tetrahedra and 10  $\text{PO}_4$  tetrahedra. Such structural units (Fig. 3) exhibit close relationships with the carnegite structure  $\text{NaAlSiO}_4$  (Ref. 5). In both frameworks, each  $\text{AlO}_4$  tetrahedron shares its four apices with  $\text{PO}_4$  (or  $\text{SiO}_4$ ) tetrahedra so that the 2 tetrahedra  $\text{AlO}_4$  and  $\text{PO}_4$  (or  $\text{SiO}_4$ ) forming the  $\text{AlPO}_7$  (or  $\text{AlSiO}_7$ )

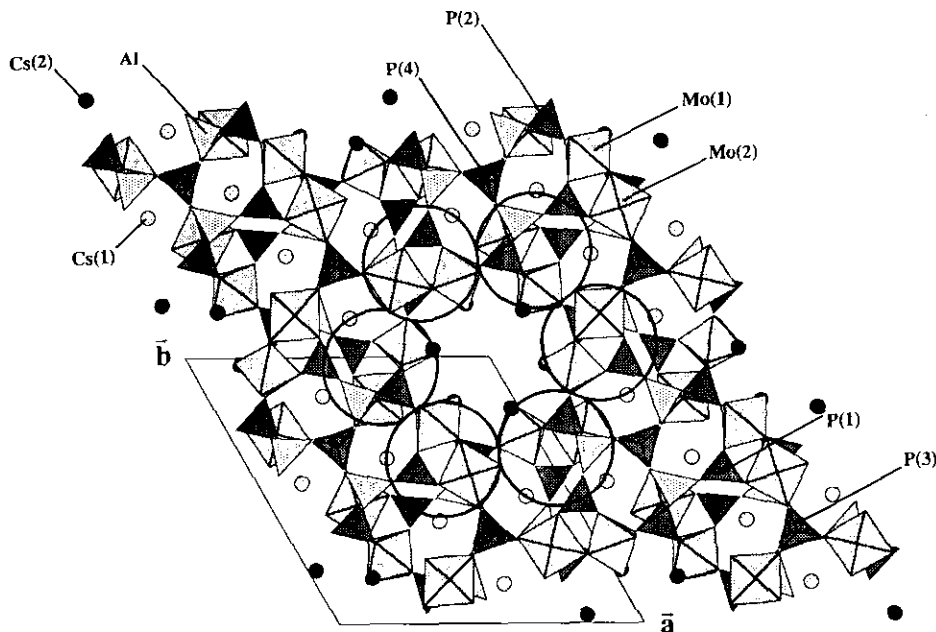


FIG. 1. Projection of the structure along  $c$ , showing the two kinds of tunnels and the  $[\text{AlMo}_3\text{P}_3\text{O}_{22}]_x$  columns (circled).

groups exhibit a staggered configuration. Nevertheless, the  $\text{AlPO}_7$  groups are significantly tilted with respect to each other compared to the  $\text{AlSiO}_7$  groups in the carnegite structure due to the strains induced by the  $\text{MoO}_6$  octahedra.

The geometry of the  $\text{AlO}_4$  tetrahedron is rather regular, similar to that observed in carnegite (5) and in  $\text{MoAlP}_2\text{O}_9$  (6), with Al–O distances ranging from 1.715 to 1.738 Å (Table 4). Four independent  $\text{PO}_4$  tetrahedra must be distinguished, labeled P(1), P(2), P(3), and P(4); three of them, P(1), P(2), and P(4), form the “ $\text{Al}_3\text{P}_{10}\text{O}_{40}$ ” unit, whereas P(3) is a monophosphate group. The P(1) tetrahedron that shares one apex with one  $\text{AlO}_4$  tetrahedron and three other apices with the same “ $\text{Mo}_3\text{O}_{15}$ ” octahedral unit (Fig. 4a) is regular, with distances ranging from 1.518 to 1.542 Å (Table 4). The P(2) tetrahedron that shares one apex with one  $\text{AlO}_4$  tetrahedron, two apices with the same “ $\text{Mo}_3\text{O}_{15}$ ” unit, and one apex with another “ $\text{Mo}_3\text{O}_{15}$ ” unit (Fig. 4b) is less regular with three distances ranging from

1.509 to 1.518 Å, and a significantly larger one, P–O(4) of 1.550 Å (Table 4); this larger distance can be explained by the fact that O(4) has two Cs(1) nearest neighbors. The two remaining phosphorous atoms, P(3) and P(4), are statistically distributed over two split, half-occupied positions. P(3) and P(4) atoms alternate in an alignment along  $c$ , leading to two possibilities for the orientation of the  $\text{PO}_4$  tetrahedra:

- (i) all the tetrahedra of one row are pointing their free

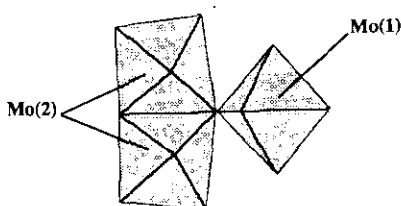


FIG. 2. The  $\text{Mo}_3\text{O}_{15}$  octahedral unit.

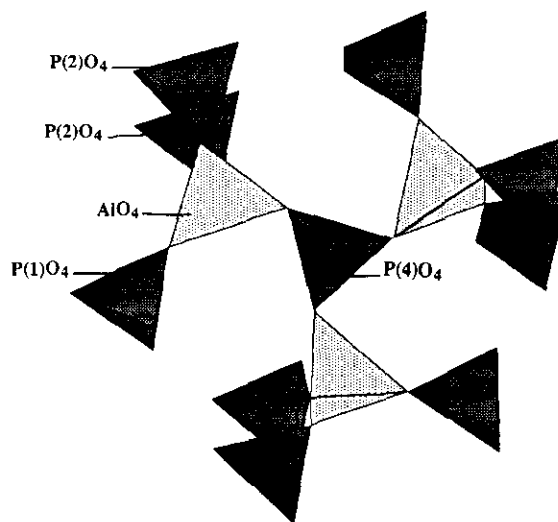


FIG. 3. The  $\text{Al}_3\text{P}_{10}\text{O}_{40}$  tetrahedral unit composed of 3  $\text{AlO}_4$  tetrahedra and 10  $\text{PO}_4$  tetrahedra.

**TABLE 4**  
Distances (Å) and Angles (°) in the Polyhedra

<b>Mo(1)</b>	O(1)	O(2)	O(3)	O(4)	O(4 <sup>i</sup> )	O(5)
O(1)	1.670(7)	2.76(1)	2.76(1)	2.747(7)	2.747(7)	3.80(1)
O(2)	96.7(4)	2.014(8)	4.04(1)	2.81(1)	2.81(1)	2.77(1)
O(3)	95.2(3)	168.1(3)	2.051(7)	2.879(7)	2.879(7)	2.807(9)
O(4)	96.0(2)	88.6(2)	90.2(2)	2.015(5)	4.01(1)	2.775(7)
O(4 <sup>i</sup> )	96.0(2)	88.6(2)	90.2(2)	168.0(3)	2.015(5)	2.775(7)
O(5)	179.5(3)	83.8(3)	84.3(3)	84.0(2)	84.0(2)	2.129(7)
<b>Mo(2)</b>	O(3)	O(6)	O(7)	O(8)	O(9)	O(10)
O(3)	2.051(5)	2.813(8)	3.011(6)	4.05(1)	2.97(1)	2.734(8)
O(6)	96.9(3)	1.696(6)	2.733(8)	2.863(8)	2.765(9)	3.86(1)
O(7)	93.6(2)	92.2(3)	2.079(5)	2.675(7)	3.96(1)	2.730(7)
O(8)	163.0(3)	99.4(3)	80.8(2)	2.047(5)	2.696(5)	2.782(7)
O(9)	96.7(2)	99.6(3)	163.3(3)	85.6(2)	1.920(6)	2.865(9)
O(10)	80.7(2)	171.6(3)	79.9(2)	82.5(2)	88.7(3)	2.170(5)
	<b>P(1)</b>	O(5)	O(10)	O(10 <sup>i</sup> )	O(11)	
	O(5)	1.542(7)	2.511(8)	2.511(8)	2.48(1)	
	O(10)	109.8(3)	1.528(5)	2.50(1)	2.505(8)	
	O(10 <sup>i</sup> )	109.8(3)	109.9(4)	1.528(5)	2.505(8)	
	O(11)	107.4(4)	110.0(3)	110.0(3)	1.531(8)	
	<b>P(2)</b>	O(4 <sup>ii</sup> )	O(7 <sup>ii</sup> )	O(8)	O(12)	
	O(4 <sup>ii</sup> )	1.550(5)	2.524(7)	2.464(7)	2.451(7)	
	O(7 <sup>ii</sup> )	111.2(3)	1.509(5)	2.496(7)	2.450(8)	
	O(8)	106.9(3)	111.1(3)	1.518(5)	2.521(7)	
	O(12)	106.4(3)	108.5(3)	111.7(3)	1.510(6)	
	<b>P(3)</b>	O(2 <sup>iii</sup> )	O(2 <sup>ii</sup> )	O(2 <sup>iv</sup> )	O(13)	
	O(2 <sup>iii</sup> )	1.506(8)	2.50(1)	2.50(1)	2.40(2)	
	O(2 <sup>ii</sup> )	112.2(2)	1.506(8)	2.50(1)	2.40(2)	
	O(2 <sup>iv</sup> )	112.2(2)	112.2(2)	1.506(8)	2.40(2)	
	O(13)	106.6(2)	106.6(2)	106.6(2)	1.49(2)	
	<b>P(4)</b>	O(14)	O(14 <sup>v</sup> )	O(14 <sup>vi</sup> )	O(15)	
	O(14)	1.522(8)	2.47(2)	2.47(2)	2.48(2)	
	O(14 <sup>v</sup> )	108.7(3)	1.522(8)	2.47(2)	2.48(2)	
	O(14 <sup>vi</sup> )	108.7(3)	108.7(3)	1.522(8)	2.48(2)	
	O(15)	110.2(3)	110.2(3)	110.2(3)	1.50(3)	
	<b>Al</b>	O(11 <sup>vii</sup> )	O(12)	O(12 <sup>i</sup> )	O(14 <sup>i</sup> )	
	O(11 <sup>vii</sup> )	1.738(8)	2.713(9)	2.713(9)	2.85(1)	
	O(12)	103.0(3)	1.730(6)	3.03(1)	2.796(9)	
	O(12 <sup>i</sup> )	103.0(3)	122.2(4)	1.730(6)	2.796(9)	
	O(14 <sup>i</sup> )	111.4(4)	108.5(3)	108.5(3)	1.715(9)	
	Cs(1)–O(1)	= 3.261(5)		Cs(2)–O(1)	= 3.117(8)	
	Cs(1)–O(2 <sup>vi</sup> )	= 3.378(6)		Cs(2)–O(3)	= 3.338(7)	
	Cs(1)–O(4)	= 3.305(5)		Cs(2)–O(6)	= 3.212(8)	
	Cs(1)–O(4 <sup>vi</sup> )	= 3.093(5)		Cs(2)–O(6 <sup>ix</sup> )	= 3.280(8)	
	Cs(1)–O(5 <sup>vi</sup> )	= 3.153(4)		Cs(2)–O(6 <sup>i</sup> )	= 3.367(9)	
	Cs(1)–O(8 <sup>viii</sup> )	= 3.299(6)		Cs(2)–O(6 <sup>x</sup> )	= 3.432(9)	
	Cs(1)–O(10 <sup>viii</sup> )	= 2.870(5)		Cs(2)–O(7 <sup>viii</sup> )	= 3.391(12)	
	Cs(1)–O(13 <sup>iii</sup> )	= 2.896(4)		Cs(2)–O(9 <sup>ix</sup> )	= 3.133(8)	
	Cs(1)–O(15)	= 3.217(11)				

*Note.* Symmetry code: (i)  $x, y, 1/2 - z$ ; (ii)  $y, y - x, 1 - z$ ; (iii)  $1 - x, 1 - y, 1 - z$ ; (iv)  $1 + x - y, x, 1 - z$ ; (v)  $1 - y, 1 + x - y, z$ ; (vi)  $y - x, 1 - x, z$ ; (vii)  $1 - y, x - y, z$ ; (viii)  $x - y, x, 1 - z$ ; (ix)  $-y, x - y, z$ ; and (x)  $-y, x - y, 1/2 - z$ .

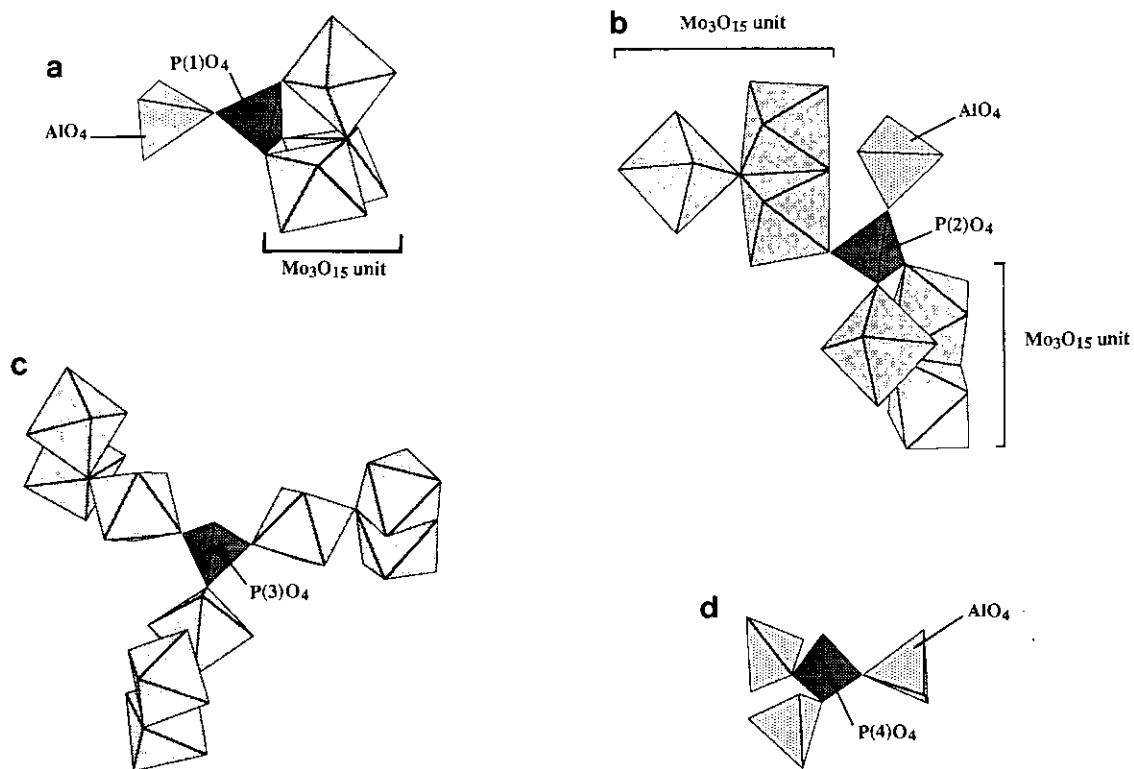


FIG. 4.  $\text{PO}_4$  tetrahedra environments: (a)  $\text{P}(1)\text{O}_4$  tetrahedron, sharing one apex with one  $\text{AlO}_4$  tetrahedron and three apices with one  $\text{Mo}_3\text{O}_{15}$  unit; (b)  $\text{P}(2)\text{O}_4$  tetrahedron, sharing one apex with one  $\text{AlO}_4$  tetrahedron, two apices with the same  $\text{Mo}_3\text{O}_{15}$  unit, and one apex with another  $\text{Mo}_3\text{O}_{15}$  unit; (c)  $\text{P}(3)\text{O}_4$  tetrahedron, linked to three  $\text{Mo}_3\text{O}_{15}$  units, its fourth corner being free; and (d)  $\text{P}(4)\text{O}_4$  tetrahedron, linked to three  $\text{AlO}_4$  tetrahedra, its fourth corner being free.

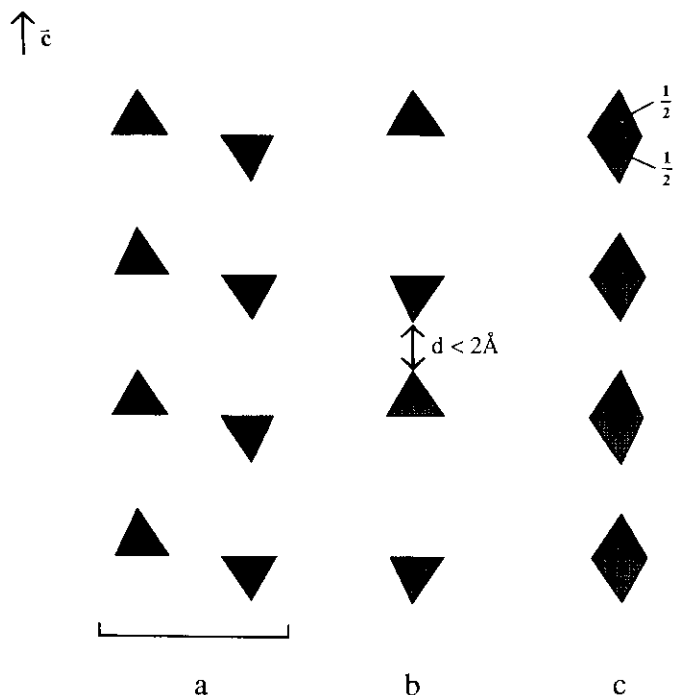


FIG. 5. Possible orientations for the  $\text{P}(3)$  and  $\text{P}(4)$  tetrahedra: (a) all the tetrahedra are pointing their free corner in the same direction; (b) one tetrahedron pointing up alternates with one tetrahedron pointing down; and (c) random occupancy with half-occupied sites.

corner in the same direction, i.e., all up or all down (Fig. 5a); and

(ii) there is alternatively one tetrahedron pointing up and one tetrahedron pointing down (Fig. 5b).

The second hypothesis would imply an O–O distance between two free apices smaller than  $2 \text{ \AA}$  and is ruled out. Consequently one can explain the structural results by the fact that in one row all the  $\text{PO}_4$  tetrahedra point their free corners in the same direction but that phenomenon is not consistent from one row to the others throughout the crystal; thus, the rows of  $\text{PO}_4$  tetrahedra pointing their corners in opposite directions along  $c$  are distributed statistically, leading to an apparent random occupancy of the split  $\text{P}(3)$  and  $\text{P}(4)$  sites in the unit cell, and the corresponding O(13) and O(15) sites are also statistically half-occupied (Fig. 5c). Note that the  $\text{P}(3)$  tetrahedron which is linked to three different “ $\text{Mo}_3\text{O}_{15}$ ” units (Fig. 4c), exhibits three corresponding identical P–O distances ( $1.506 \text{ \AA}$ ); the fourth P–O bond that corresponds to the free oxygen is slightly smaller ( $1.49 \text{ \AA}$ ) (Table 4). In the same way, the  $\text{P}(4)$  tetrahedron, which is linked to three  $\text{AlO}_4$  tetrahedra (Fig. 4d) exhibits three identical P–O bonds ( $1.522 \text{ \AA}$ ), the fourth corresponding to its smaller free oxygen apex ( $1.50 \text{ \AA}$ ) (Table 4).

Thus the entire  $[\text{Mo}_9\text{Al}_3\text{P}_{11}\text{O}_{39}]_\infty$  host lattice can be de-

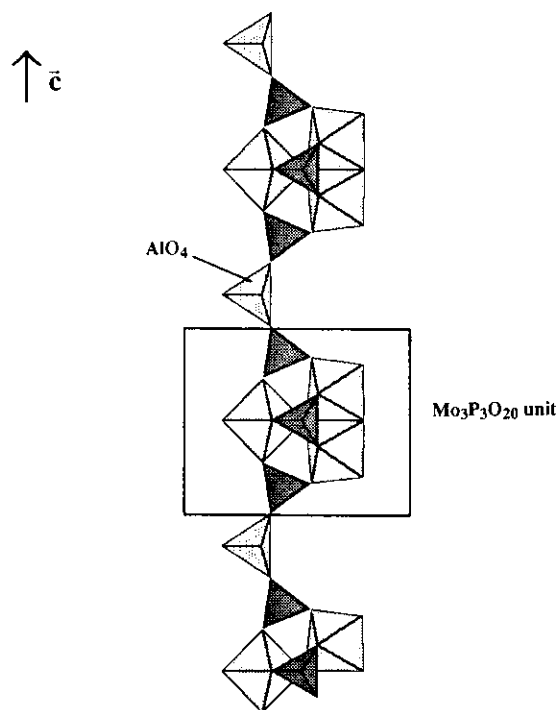


FIG. 6.  $[\text{AlMo}_3\text{P}_3\text{O}_{22}]_\infty$  column built from  $\text{Mo}_3\text{P}_3\text{O}_{20}$  units connected through  $\text{AlO}_4$  tetrahedron.

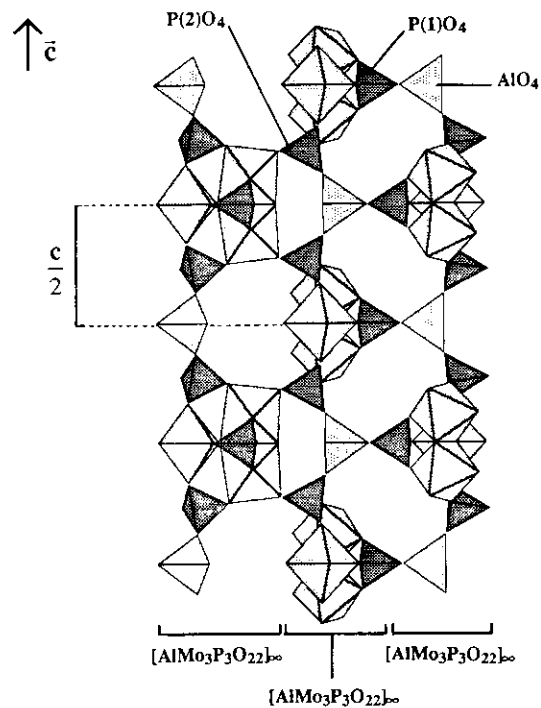


FIG. 7. Connection of  $[\text{AlMo}_3\text{P}_3\text{O}_{22}]_\infty$  columns.

scribed as the association of three kinds of units, octahedral " $\text{Mo}_3\text{O}_{15}$ " units, tetrahedral " $\text{Al}_3\text{P}_{10}\text{O}_{40}$ " units, and single  $\text{PO}_4$  tetrahedra that share the corners of their polyhedra in three different ways: (i) one  $\text{PO}_4$  tetrahedron of the  $\text{Al}_3\text{P}_{10}\text{O}_{40}$  unit shares three apices with the  $\text{MoO}_6$  octahedra of the same  $\text{Mo}_3\text{O}_{15}$  unit; (ii) one  $\text{PO}_4$  tetrahedron of the  $\text{Al}_3\text{P}_{10}\text{O}_{40}$  unit shares two apices with the same  $\text{Mo}_3\text{O}_{15}$  unit and one apex with another one, and (iii) one single  $\text{PO}_4$  tetrahedron (P(3)) that is connected to three different  $\text{Mo}_3\text{O}_{15}$  units.

In this structure one also recognizes " $\text{Mo}_3\text{P}_3\text{O}_{20}$ " units (Fig. 6) composed of one " $\text{Mo}_3\text{O}_{15}$ " unit sharing its apices with three  $\text{PO}_4$  tetrahedra (P(1) and P(2)) similar to those encountered in  $\text{Cs}_6\text{Mo}_7\text{O}_9(\text{PO}_4)_7 \cdot \text{H}_2\text{O}$  (Ref. 3). Such trimetric " $\text{Mo}_3\text{P}_3\text{O}_{15}$ " units are connected along  $c$  through  $\text{AlO}_4$  tetrahedra so that they form  $[\text{AlMo}_3\text{P}_3\text{O}_{22}]_\infty$  columns running along that direction (Fig. 6). The whole structure can thus be described as the assemblage of these columns through the corners of their polyhedra and through two kinds of  $\text{PO}_4$  tetrahedra P(3) and P(4). From Fig. 1, one

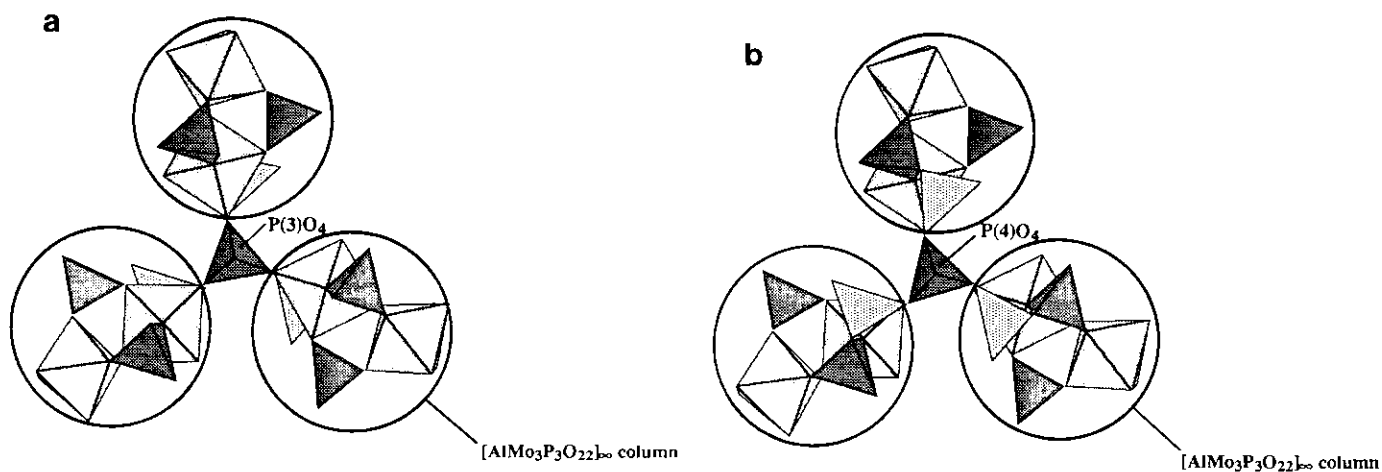


FIG. 8. P(3) $\text{O}_4$  tetrahedron sharing three apices with the  $\text{MoO}_6$  octahedra of three different columns (circled) and (b) P(4) $\text{O}_4$  tetrahedron sharing three apices with the  $\text{AlO}_4$  tetrahedra of three different columns (circled).

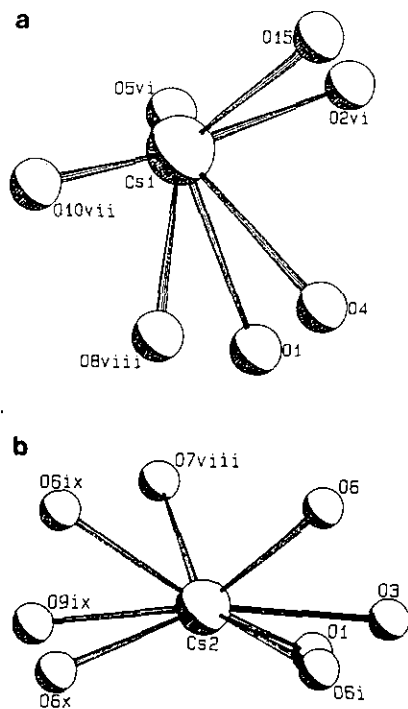


FIG. 9. The cesium environment.

indeed observes that six columns (circled) surrounding one large tunnel share the corners of their polyhedra in such a way that one P(2) tetrahedron is connected with one Mo(2) of the other column, and that one P(1) tetrahedron of one column is linked to one  $\text{AlO}_4$  tetrahedron of the adjacent column (Fig. 7). As a result, two adjacent columns are oriented at a  $120^\circ$  angle and are shifted  $c/2$  with respect to each other. In the same way, it can easily be seen that each P(3) tetrahedron shares three apices with the  $\text{MoO}_6$  octahedra of three different columns,

whereas each P(4) tetrahedron is connected to the  $\text{AlO}_4$  tetrahedra of three different columns (Figs. 1 and 8b). The Cs(1) cations, located in the smaller tunnels (Fig. 1), are surrounded by eight oxygen atoms (Fig. 9a) at Cs(1)–O distances ranging from 2.870 to 3.378 Å. Note that one of them can be either O(13) or O(15) because of the two possible orientations of P(3) and P(4) tetrahedra which prevent the simultaneous presence of O(13) and O(15) in the Cs(1) cation environment.

The Cs(2) cations that belong to the large tunnels (Fig. 1) are in fact located near the wall of the latter, more exactly in adjacent cages. They are surrounded by eight oxygen atoms (Fig. 9b) with rather large Cs–O distances ranging from 3.117 to 3.432 Å (Table 4) that explain the high thermal factor obtained for these cations.

In conclusion, the compound  $\text{Cs}_9\text{Mo}_9\text{Al}_3\text{P}_{11}\text{O}_{59}$  represents the second aluminophosphate of Mo(V), besides  $\text{MoAlP}_2\text{O}_9$  (6), that has been synthesized thus far. This confirms that aluminium is a good candidate for the stabilization of mixed frameworks involving pentavalent molybdenum. The existence of large tunnels and cages in this structure suggests that it should be possible to synthesize other Mo(V) monophosphates with an open structure, varying the nature of the invited cation and also the molar ratios of the elements that participate to the host lattice.

## REFERENCES

1. R. C. Haushalter and L. A. Mundi, *Chem. Mater.* **4**, 31 (1992).
2. G. Costentin, A. Leclaire, M. M. Borel, A. Grandin, and B. Raveau, *Rev. Inorg. Chem.* **13**, 77 (1993).
3. A. Guesdon, M. M. Borel, A. Leclaire, A. Grandin, and B. Raveau, *J. Solid State Chem.*, **111**, 315 (1994).
4. W. H. Zachariassen, *J. Less-Common Met.* **62**, 1 (1978).
5. T. F. W. Barth and F. E. Posjak, *Z. Kristallogr.* **81**, 135 (1932).
6. A. Leclaire, M. M. Borel, A. Grandin, and B. Raveau, *Z. Kristallogr.* **190**, 135 (1990).